Differentiation (1998) 63:21–32

ORIGINAL ARTICLE

Sabine Kloth · Tanja Gmeiner · Joachim Aigner
Michael L. Jennings · W. Röckl · Will W. Minuth

Transitional stages in the development of the rabbit renal collecting duct

Accepted in revised form: 21 January 1998

Abstract The collecting duct (CD) epithelium of the mammalian kidney is an extraordinary structure with respect to its functional changes during development and its heterogeneous composition when matured. All of the different nephron epithelia of the mammalian kidney consist of one single cell type. In contrast, the differentiated CD is composed of at least three distinct cell types [principal, α intercalated-, and β intercalated cells] that are responsible for the multiple physiological functions of this kidney compartment. During development the function of the CD changes: initially, the CD ampulla serves as an embryonic inducer, while the matured epithelium plays a key role in maintaining the homeostasis of body fluids. At present the process of CD maturation is not well understood. Neither the time course of development nor the morphogenic factors leading to the heterogeneously composed epithelium are known. In the present study the differentiation of the CD epithelium was investigated using newly developed monoclonal antibodies and well-characterized antisera. The morphological changes induced during differentiation were monitored by immunohistochemistry and scanning electron microscopy. The experiments were performed on neonatal and adult rabbit kidneys. Results obtained by light microscopical techniques and scanning electron microscopy revealed that the ampullary tip can be distinguished from the ampullary neck, as well as from the maturing CD. A number of proteins that were not detectable in the ampulla were detected in the neonatal CD and were found at even higher concentrations in the adult CD ($P_{CD}8$, chloride/bicarbonate exchanger). Other proteins ($P_{CD}9$) were downregulated during differentiation. For the first time the transient character of the differentiation stage of the neonatal CD could be demonstrated unequivocally. Furthermore, considerable heterogeneity in protein expression patterns ($P_{CD}6$ and $P_{CD}9$) was demonstrated within the β IC cell population of the mature CD.

S. Kloth (✉) · T. Gmeiner · J. Aigner · W.W. Minuth
Department of Anatomy,
University of Regensburg, Universitätsstrasse 31,
D-93053 Regensburg, Germany

M.L. Jennings
Department of Physiology and Biophysics,
University of Arkansas for Medical Sciences,
4301 W. Markham Street, Little Rock, AR 72205, USA

W. Röckl
GBF Braunschweig, ZWE Gene Expression, Mascheroder Weg 1,
D-38124 Braunschweig, Germany

Introduction

The renal collecting duct (CD) fulfills two very different functions. It is firstly an embryonic inducer of new nephrons [45] and then continues with the control of acid/base status [1], the sodium/potassium (Na/K) balance [7], and the water content of the organism. The mature CD epithelium is comprised of at least three different cell types [principal (P), α intercalated (α IC), and β intercalated (β IC) cells] which can be distinguished on the basis of their morphological [32] and physiological features [29, 47].

The pleiotropic action of the renal CD starts at the onset of renal organogenesis by the invasion of the uretic bud epithelium into the metanephrogenic mesenchyme [45]. This tissue interaction results first in several dichotomous branching of the bud epithelium. The blind ends are known as ampullae and trigger the subsequent permanent induction of all of the nephrons. The dichotomous dividing mechanism leads to the CD system with many arborized endings that are found beyond the capsula fibrosa in the neonatal rabbit kidney. The nephrons and the CD system continue to develop until the late neonatal period. For this reason fully embryonic CD ampullae in the outer cortex can be compared with more mature tissue in the midcortical and medullary region of the neonatal kidney.

With respect to morphology and function, three different zones can be distinguished in the CD ampulla. The ampullary tip is composed of light-staining cells [12]. In the tip region the lumen of the ampulla is broader than in the next zone, called the ampullary neck. The neck consists of several cell layers expressing a darker staining

than the cells of the tip. This region is followed by a transition zone, where the epithelium differentiates into light- and dark-staining cells [27]. Within the transition zone cells with microplicae (α IC cell) can already be distinguished from cells with long microvilli (β IC cell) or cells bearing a cilium and few stubby villi (P cell) [3]. Thus, from the ampullary tip to the cells of the neck and the transition zone, a differentiation gradient of embryonic to maturing P and IC cells is observed.

It has been assumed that the induction capability of the CD is located in the ampullary tip epithelium [19, 45]. This is supported by the fact that within the ampullary neck we can already observe the first morphological signs of differentiation [4]. Furthermore, the neck portion of the ampulla is the site where multiple cell divisions take place, causing the epithelium to grow towards the capsula fibrosa by elongation rather like a telescope antenna [39]. Then, in the transition zone, the sudden appearance of at least three distinct cell types is observed [4, 27]. According to morphological criteria, the α- and β-type IC and P cells become visible in this region [3, 4]. To date little knowledge is available about the morphogenic factors influencing the differentiation from the embryonic inducer epithelium into the functional tissue of the mature kidney [15, 42].

In the present experiments we utilized immunohistochemical methods to investigate the individual changes of the embryonic CD cells into the functional epithelium. One major problem was a lack of markers to identify the various cell types during functional differentiation. Morphological [32] and physiological [29, 46, 47] data revealed that the different cell types within the CD represent very distinct cell populations. This was confirmed by some histochemical results. However, immunohistochemical experiments showed that the different cell types also share common characteristics. Thus, three different categories of immunolabelling patterns were described in the literature (Table 1). The first group comprised markers abundant on a single cell type, such as the amiloride-sensitive Na channel on P cells, peanut agglutinin (PNA) binding on the β-type IC cells, or the basolateral expression of the chloride/bicarbonate (Cl/HCO_3) exchanger by α IC cells. The second group includes markers that label not only P or one of the different types of IC cells, but were found on P cells as well as on one IC cell type or were expressed by both IC cell types. Within the third group are the markers that bind to all types of CD cells. As shown in Table 1, immunohistochemical studies can demonstrate both the similarities and the differences between the different types of CD cells. At present the origin of the different cell types is not clear. For this reason we were interested in investigating the immunohistochemical differentiation pattern of the developing CD. The newly generated monoclonal antibodies reacting with the CD antigens $P_{CD}6$, $P_{CD}8$, and $P_{CD}9$ were used in conjunction with the monoclonal antibody IVF12, which detects the Cl/HCO_3 exchanger [22]. With these markers we traced the development of the CD epithelium from embryonic inducer to the mature CD with its well-known functions. We found that the maturation of CD cells is characterized by the acquisition of new functional proteins as well as the transient appearance and the loss of typical features.

Materials and methods

Tissue preparation

New Zealand rabbits were anesthetized and killed by cervical dislocation. The kidneys were removed immediately and frozen in liquid nitrogen. Neonatal kidneys were obtained from 1- to 3-day-old animals. Mature organs were prepared from rabbits older than 6 months.

Production of monoclonal antibodies

The production of monoclonal antibodies has already been described in detail [26]. Homogenate from neonatal kidneys was used for the immunization of Balb/c mice. Primary immunization and two further booster injections were given intraperitoneally. Monoclonal antibodies were produced according to the method of Koehler and Milstein [28]. Spleen cells were fused with myeloma cells of the x63Ag8.653 line. The cells were cultured in RPMI 1640 (Gibco-BRL Life Technologies, Eggenstein, Germany) with 2×10^{-3} M L-glutamine (Gibco-BRL Life Technologies), 10% fetal calf serum (Boehringer, Mannheim, Germany), 1×10^{-5} M 2-mercaptoethanol (Serva, Heidelberg, Germany) in conventional culture plates or flasks (Falcon, Becton Dickinson, Heidelberg, Germany) in an incubator (37° C, 95% air/5% CO_2 atmosphere, Hereaus, Hanau, Germany). Hybridomas were cloned using a limiting dilution procedure. Culture supernatants were tested for tissue-specific antibodies by immune incubation of kidney sections.

Light microscopical techniques

Cryosections (8 μm) of neonatal rabbit kidneys and renal explants were cut with a cryomicrotome (Microm, Heidelberg, Germany). Two different methods were used for antigen detection. In the first set of experiments a modified immunoperoxidase method described by Kujat et al. [30] was applied. Sections were fixed according to a two-step fixation protocol. First the sections were incubated for 30 s in a solution of 4.2% paraformaldehyde (Merck, Darmstadt, Germany), 16% picric acid (Fluka, Buchs, Switzerland), 0.002% cobalt chloride, and 0.1% glutaraldehyde (Serva) in phosphate-buffered saline (PBS), pH 7.2. Subsequently, the sections were immersed for 15 min in a solution that included all the reagents listed above except glutaraldehyde. Following a washing and blocking step, primary antibodies were applied overnight. A biotin-conjugated donkey anti-mouse immunoglobulin (1:600, Dianova, Hamburg, Germany) served as detecting antibody. In order to block endogneous peroxidases, the sections were washed and incubated for 30 min in phenylhydrazine solution (Sigma, Deisenhofen, Germany) including 0.0006% hydrogen peroxide (H_2O_2) (Merck). An avidin-biotin detection complex was then applied according to the manufacturer's instructions (Vectastain, Vector, Burlingame, USA). The enzyme reaction was started by adding the substrate solution (0.5 mg/ml diaminobenzidine, 0.1 M TRIS, pH 7.4, 0.002% cobalt chloride, 0.04% nickel chloride, 0.012% H_2O_2, Sigma) and stopped by rinsing in washing buffer. The sections were dehydrated and finally embedded in DePeX (Serva). This was the only suitable method for band 3 protein detection. The protein could not be detected after simple ethanol fixation [23].

Primary antibodies

$P_{CD}6$ (IgM), $P_{CD}8$ (IgM), and $P_{CD}9$ (IgG_1) antibodies were applied as undiluted culture supernatants. The antibody IVF12 (mouse monoclonal antibody, IgG_{2a}) was diluted 1:400 prior to application. Unrelated monoclonal antibodies or pre-immune mouse sera served as controls. As a control for non-specific binding of the detecting antibody, sections were incubated omitting the primary antibody. Neither

of these controls revealed any labelling of the CD epithelium. The number of positive or negative cells was estimated by counting longitudinal sections of CD in the cortical, midcortical, and medullary parts of the kidney. More than 100 sections were evaluated.

Co-incubation experiments

The lectin PNA has been described as a marker for the β-type IC cells of the rabbit [33]. In order to analyze whether antibody-labelled or unlabelled cells belonged to this cell type, co-incubation experiments were carried out with the antibodies $P_{CD}6$ and $P_{CD}9$ and the lectin. The fixation method described above resulted in autofluorescence of the tissue. Therefore, another fixation protocol was used for immunofluorescence detection of the P_{CD} antigens. Tissue sections were fixed in ice-cold ethanol and washed. Primary antibodies were applied for 90 min. Rhodamine-coupled antisera (Dianova) were used for the detection of bound primary antibodies. The sections were then treated with fluorescein isothiocyanate-conjugated PNA (1:2,000, Vector). Following the final washing step, the sections were mounted in FITCguard (Testoc, Chicago, Ill., USA) embedding medium and analyzed using an Axiovert microscope (filter I:450–490, FT 510, LP 520; Zeiss, Oberkochen, Germany). For documentation TriXPan film (Kodak, Hemel-Hepstead, United Kingdom) was used.

Sections incubated with $P_{CD}9$ and PNA were examined with a confocal laser scan microscope (MRC 500, BioRad, Munich, Germany; in combination with a Zeiss IM 35 microscope). The optical sections were processed using software from BioRad. Co-incubation experiments with IVF12 and the P_{CD} antibodies could not be performed due to the autofluorescence induced by the fixative needed for IVF12 detection.

Scanning electron microscopy

Freshly prepared kidneys were cut in small pieces. The samples were fixed with 3% glutaraldehyde solution (Serva), frozen in liquid propane, and sectioned with the cryomicrotome. The sections (35 µm) were post-fixed with 1% osmium tetroxide, washed, and dehydrated in a graded series of ethanol, critical point dried with CO_2, and sputter-coated with gold. The specimens were examined with a DSM 940 A microscope (Zeiss).

Biochemical analysis of renal antigens

For the preparation of tissue homogenate, kidneys of neonatal rabbits were homogenized in ice-cold buffer (1×10^{-2} M TRIS-[hydrocylmethyl]-aminomethane, 0.15 M NaCl, 9×10^{-3} M EDTA, 1×10^{-5} M phenylmethane sulfonyl fluoride, Sigma). Homogenates were centrifuged (15 min, 12,000×*g*), supernatants discarded, and the pellet resuspended in buffer containing 2% Triton X-100 (Sigma). After 10 min incubation the lysate was centrifuged once again (30 min, 12,000×*g*). Aliquots of the lysate (20 µg protein/lane) were used for sodium dodecyl sulfate polyacrylamide gel electrophoresis (SDS-PAGE) (10% gel) according to the method described by Laemmli [31] and for two-dimensional electrophoresis according to the protocol of O'Farrell [40]. For the first dimension of the two-dimensional electrophoresis an ampholine mixture consisting of Ampholyte pH 3.5–9.0 and pH 4.0–6.5 was used (Ampholyte, Pharmacia, Freiburg, Germany).

Separated proteins were transferred onto Immobilon P membranes (0.45 µm, Millipore, Eschborn, Germany) using a semidry blotting apparatus (PHASE, Mölln, Germany) and a discontinuous buffer system. In order to detect immunoreactive material, the blots were first blocked (PBS, pH 7.2; 0.05% Tween 20, Sigma; 10% horse serum, Boehringer), and then primary antibodies were applied as undiluted culture supernatants for 1 h. A horseradish peroxidase-conjugated donkey anti-mouse immunoglobulin antiserum (1:2,000, Dianova) served as detecting antibody. The staining reaction was started by addition of 0.5 mg/ml diaminobenzidine, 0.02% H_2O_2, and 0.03% cobalt chloride dissolved in citrate buffer, pH 6.3. The reaction was stopped by washing the membrane in tap water.

Results

Characterization of antibodies labelling CD epithelium

The mature CD epithelium is characterized by a heterogeneous cellular composition (Table 1). The different cell types can be distinguished by their diverse morphological [32] and funtional features [46]. Already in the neonatal kidney light P cells that bear a single cilium and

Table 1 Common and differential features of differentiated renal collecting duct (CD) cells (*P* principal, *IC* intercalated; – negative, + all cells express protein, (+) a proportion of cells express protein)

Category	Features	P-cell	α-Type IC cell	β-Type IC cell	Reference
1	Na channel amiloride-sensitive	+	–	–	Brown et al. 1989 [10]
1	Aquaporin-2	+	–	–	Yasui et al. 1996 [54]
1	Peanut agglutinin (PNA)	–	–	+	LeHir et al. 1982 [33]
1	Cl^-/HCO_3^- exchanger basal	–	+	–	Verlander et al. 1988 [51]
1	Cl^-/HCO_3^- exchanger apical		–	+	van Adelsberg et al. 1993 [7]
1	H^+-ATPase, apical	–	+	–	Alper et al. 1989 [6]
1	H^+-ATPase, basal		–	+	Verlander et al. 1994 [52]
2	Carbonic anhydrase II	–	+	+	Madsen et al. 1989 [34] Breton et al. 1995 [8]
2	Ecto-5-nucleotidase	–	+	+	Gandhi et al. 1990 [17]
2	Mab 503 antigen	–	+	+	Jamous et al. 1995 [21]
2	P_{CD} IV/2	+	–	+	Gilbert et al. 1990 [18]
2	$P_{CD}6$ antigen	+	+	(+)	Present study
2	$P_{CD}9$ antigen	(+)	(+)	(+)	Present study
3	Na/K-ATPase	+	+	+	Ridderstrale et al. 1988 [41]
3	Na/H exchanger	+	+	+	Weiner and Hamm 1990 [53]
3	Cytokeratin 19	+	+	+	Moll et al. 1991 [38]
3	$P_{CD}1$–5 antigens	+	+	+	Minuth et al. 1989 [37]
3	$P_{CD}8$ antigen	+	+	+	Kloth et al. 1993 [27]

[a] Category 1, proteins specific for individual cell population within the CD; category 2, proteins specific for at least two mixed cell populations within the CD; category 3, proteins expressed by all cells of the mature CD

short microvilli at the apical cell pole (Fig. 1a, d) are located side by side with dark-staining IC cells characterized by numerous long microvilli (β type) or microplicae (α type, Fig. 1c). Within the transition zone of the neonatal CD cells were observed which bore a single cilium and microplicae (Fig. 1b). These cells were found only in the neonatal and never in the adult CD.

Physiological experiments have revealed that the different cell types fulfill different functions that are associated with the expression of distinct membrane proteins and enzymes. However, monoclonal antibodies specific for the different cell types of the CD especially in rabbit kidney, are scarce. There is only one well-characterized antibody that exhibits exclusive specificity for a single cell type. α IC cells are labelled by the antibody IVF12 that binds to the Cl/HCO_3 exchanger protein, also known as the band 3 protein of the erythrocytes [22]. Therefore, we produced new monoclonal antibodies able to discriminate between the various cells of the CD epithelium. Three hybridomas ($P_{CD}6$, $P_{CD}8$, $P_{CD}9$) were cloned and further characterized. The antibodies $P_{CD}6$ (IgM) and $P_{CD}8$ (IgM) nearly exclusively labelled the CD epithelium. Only a few cells of the connecting tubule were positive for these antibodies. $P_{CD}9$ (IgGl) showed an intense reaction with cells of the CD but also reacted with cells of Bowman's capsule, interstitial cells, and the endothelium. P_{CD} antigen detection was not negatively influenced by the different fixation protocols applied in this study. All fixatives gave comparable and good results. In contrast, the band 3 protein could not be detected after simple ethanol fixation [22].

A first biochemical characterization of the antigens was carried out using kidney homogenates separated by SDS-PAGE. For immune incubation the proteins were transferred onto blot membranes. The diffuse reaction pattern of $P_{CD}6$ and $P_{CD}8$ could not be associated with distinct bands (not shown). It appeared as a braod smear covering the complete lane.

The antibody $P_{CD}9$ detected antigens migrating at 32 and 39 kilodalton (kDa) (Fig. 2a). Following two-dimensional electrophoretic separation, these bands were subdivided into several immunoreactive spots with different isoelectric points (Fig. 2b). The 39-kDa antigen was separated into four distinct spots with isolelectric points of 6.3, 6.4, 6.6, and 6.9. Under the applied experimental

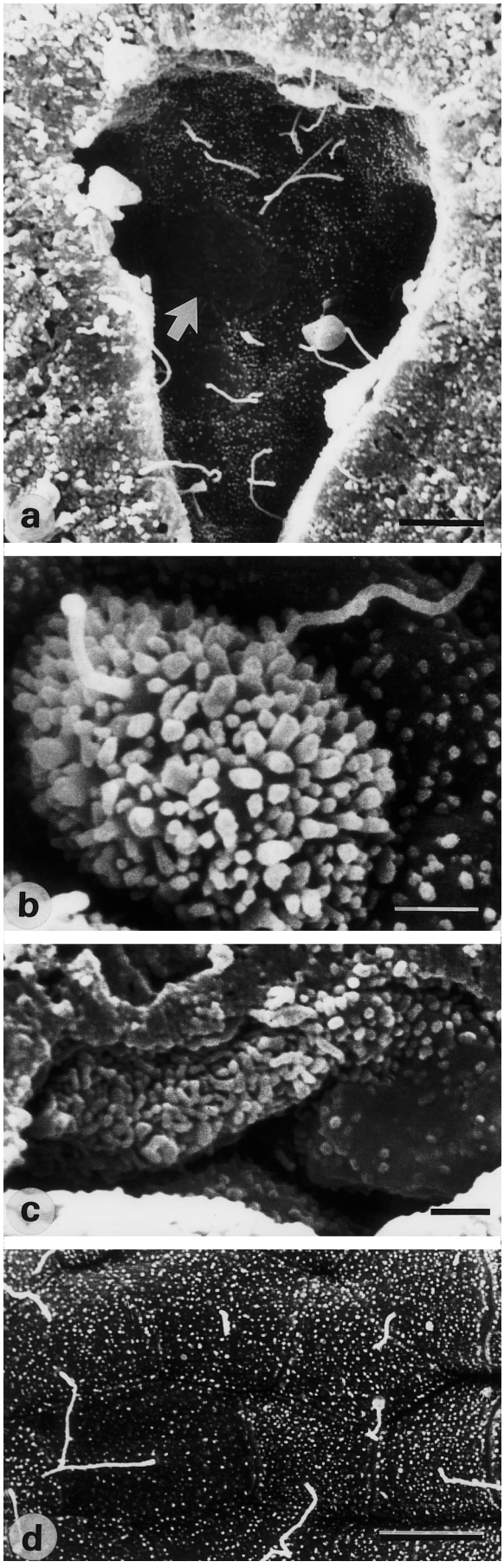

Fig. 1a–d Scanning electron microscopic analysis of the collecting duct (CD) epithelium of the neonatal kidney. **a** A CD ampulla is shown. Most cells resembled mature principal (P) cells and bore a long, single cilium and few stubby microvilli. A small number of cells with a smooth surface were found (*arrow*), which were not observed in the mature CD epithelium. *Scale bar*, 5 µm. **b** The cell shown here bears numerous long microvilli and a cilium. These cells were only detected in the neonatal CD – never in the matured epithelium. *Scale bar*, 1 µm. **c** Cells expressing typical morphological features of α intercalated (IC) cells were first found within the transition zone. α IC cells are characterized by numerous microplicae on their apical surface. *Scale bar*, 1 µm. **d** The medullary CD epithelium consisted of cells with P cell characteristics. P cells bear a long single cilium and only a few microvilli. *Scale bar*, 5 µm

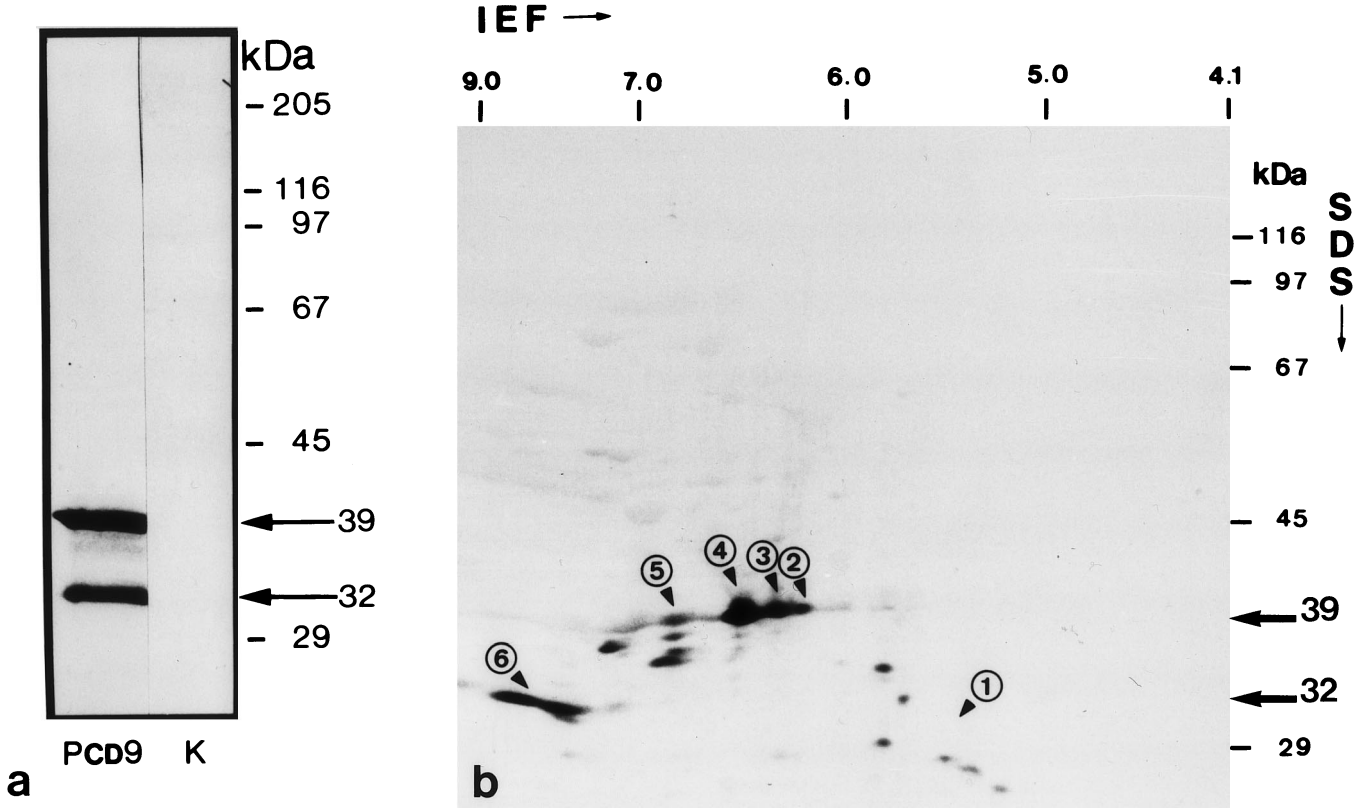

Fig. 2a, b Biochemical characterization of the $P_{CD}9$ antigens. **a** Kidney homogenate was separated under reducing electrophoretic conditions. Two bands migrating at 39 and 32 kilodaltons (*kDa*) were detected by the monoclonal antibody $P_{CD}9$ in Western blots (*first lane*). *Second lane*, the control blot was incubated only with enzyme-conjugated antibody. **b** Following two-dimensional separation of kidney homogenate the 39-kDa variant was separated into four distinct spots (numbers 2–5) within a pl range of 6.3–6.9. The 32-kDa form showed a basic pl (spot number 6). It could not be further separated under the applied conditions. Several immunoreactive spots of lower molecular weight were also detected by the $P_{CD}9$ antibody. These spots were not labelled in control blots. It is assumed that they represent proteolytic breakdown products of the 32- and 39-kDa proteins

conditions, the 32-kDa antigen migrated in the range of pI 8–9 and could not be further separated. The blot showed several other spots with aberrant molecular weights. Due to the negative reaction on control blots (not shown), we assume that these spots represent proteolytic breakdown products of the 39- and 32-kDa antigens.

The embryonic CD ampulla in neonatal kidney

Beyond the fibrous organ capsule of the neonatal kidney numerous blind-ending ampullae of the CD system are found (Figs. 1 and 3). Three zones can be distinguished by scanning electron microscopy (Figs. 1a and 3a) [3, 12]. First is the ampullary tip (I), which consists predominantly of cells with a single cilium and few stubby microvilli (Fig. 1a). It differentiates into the epithelium of the ampullary neck region (II), where most cells bear numerous microvilli. Beyond this zone cells can be observed expressing the morphological characteristics of mature P and IC cells (Fig. 1c, d). This region is called transition zone (III). From the ampullary tip to the transition zone cells were observed which were not found in the mature CD (Fig. 1a, b). Some ampullary cells showed a smooth surface, whereas cells of the transition zone carried numerous long microvilli as well as a long cilium. Both cell types were exclusively detected in the neonatal and never in the mature CD.

To investigate changes in the antigen expression patterns that accompany the differentiation of the CD epithelium we used the newly developed P_{CD} antibodies and the antibody IVF12, which detects the Cl/HCO_3 exchanger (Table 2). Incubation with $P_{CD}9$ revealed that all of the

Table 2 Immunohistochemical labelling of CD cells during development[a]

	Ampullary CD	Neonatal CD	Adult CD	Reference
$P_{CD}6$	–[b]	100%	>90% cortex	Present study
$P_{CD}8$	–	100%	100%	Present study
$P_{CD}9$	100%	100%	Variable	Present study
Cl/HCO_3 exchanger	–	<10%	11% cortex 50% o medulla	Verlander et al. 1988 [51], and present study

[a] Percentage of positive cells labelled by the individual antibody
[b] No labelling

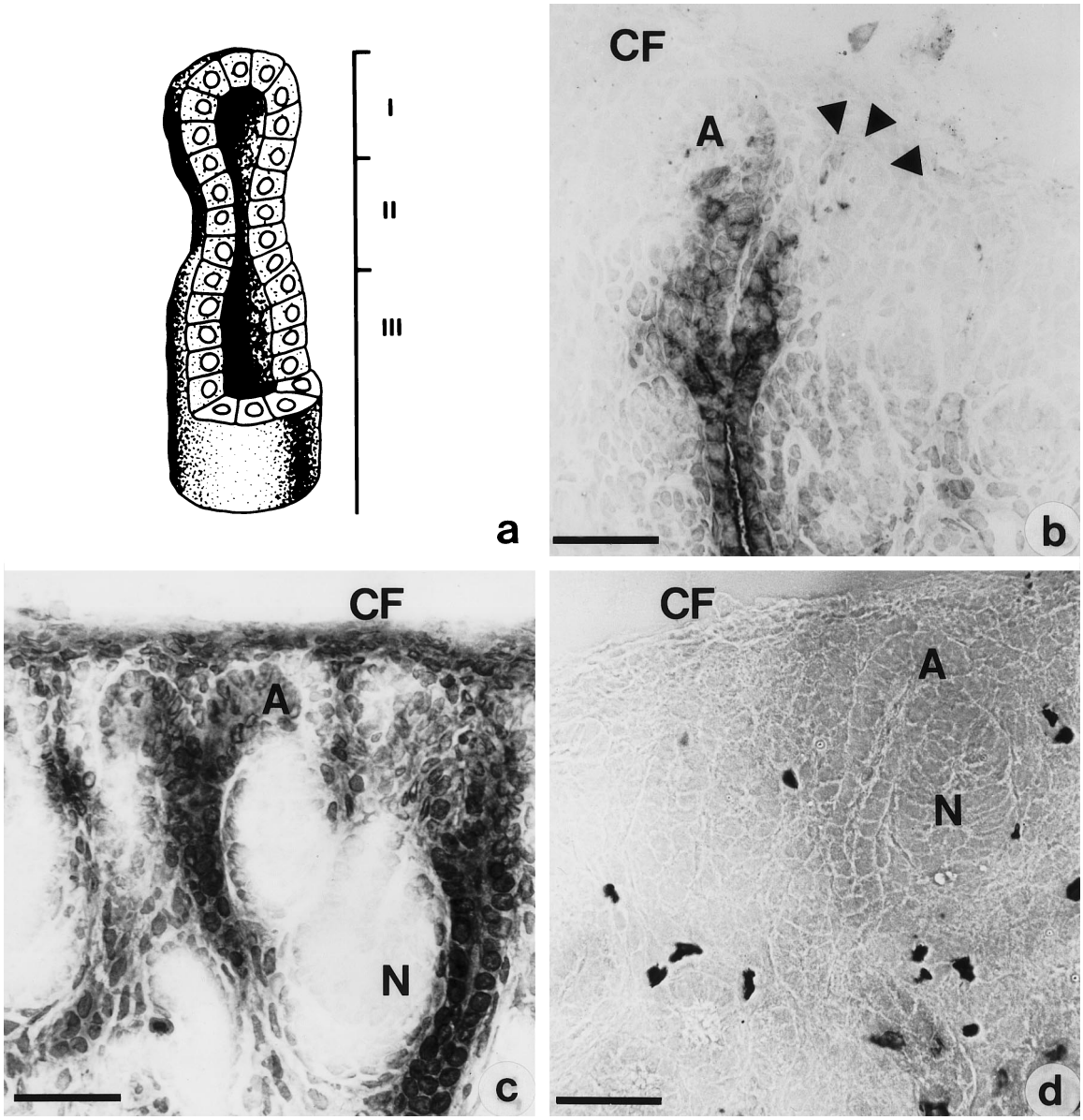

Fig. 3a–d Zonal organization of the CD ampulla. **a** The blind ends of the developing CD are called CD ampullae. The ampullae are located beneath the organ capsule. Different zones can be distinguished on the basis of morphological features. I, The ampullary tip consists of pale-staining cells that for the most part carry one single cilium and few stubby microvilli (compare with Fig. 1a). II, the ampullary neck is composed of cells that are characterized by numerous short microvilli. The majority of these cells have no cilium. III, The transition zone is located beneath the ampullary neck. Here, cells can be detected expressing the morphological features of mature CD cells. For the immune incubation experiments a sensitive indirect immunoperoxidase method was used. Primary antibodies were applied as undiluted culture supernatants. Antibody binding was detected by means of a species-specific anti-mouse antibody conjugated with biotin. Bound antibodies were detected by horseradish peroxidase-conjugated streptavidin. **b** Cells of the ampullary tip (*A*, *arrowheads*) were not labelled by the monoclonal antibody $P_{CD}6$, while cells of the ampullary neck and those of the transition zone strongly bind $P_{CD}6$. **c** All ampullae were completely labelled by $P_{CD}9$. **d** Only erythrocytes were labelled by the monoclonal antibody IVF12. No ampullary cells were detected expressing the band 3 protein. CF, Fibrous organ capsule, *N*, developing nephron. *Scale bar*, 50 µm

ampullary cells expressed this antigen (Fig. 3c). In contrast, incubation with $P_{CD}6$ (Fig. 3b) and $P_{CD}8$ showed that the tip of the ampulla was negative, while the ampullary neck gave a slight reaction and the transition zone was intensely labelled. A completely different result was obtained with the antibody IVF12 (Fig. 3d). All of the ampullary cells including tip, neck, and transition zone were negative. Thus, a time-dependent gradient of early and late-appevaring proteins was demonstrated in the CD ampulla with the monoclonal antibodies used in this study. Furthermore, the antibody $P_{CD}8$ enabled for the first time a clear-cut distinction between embryonic and further matured CD epithelium. Ampullary cells were negative for $P_{CD}8$ labelling, while the cells of the neck and transition zone became positive for this antigen.

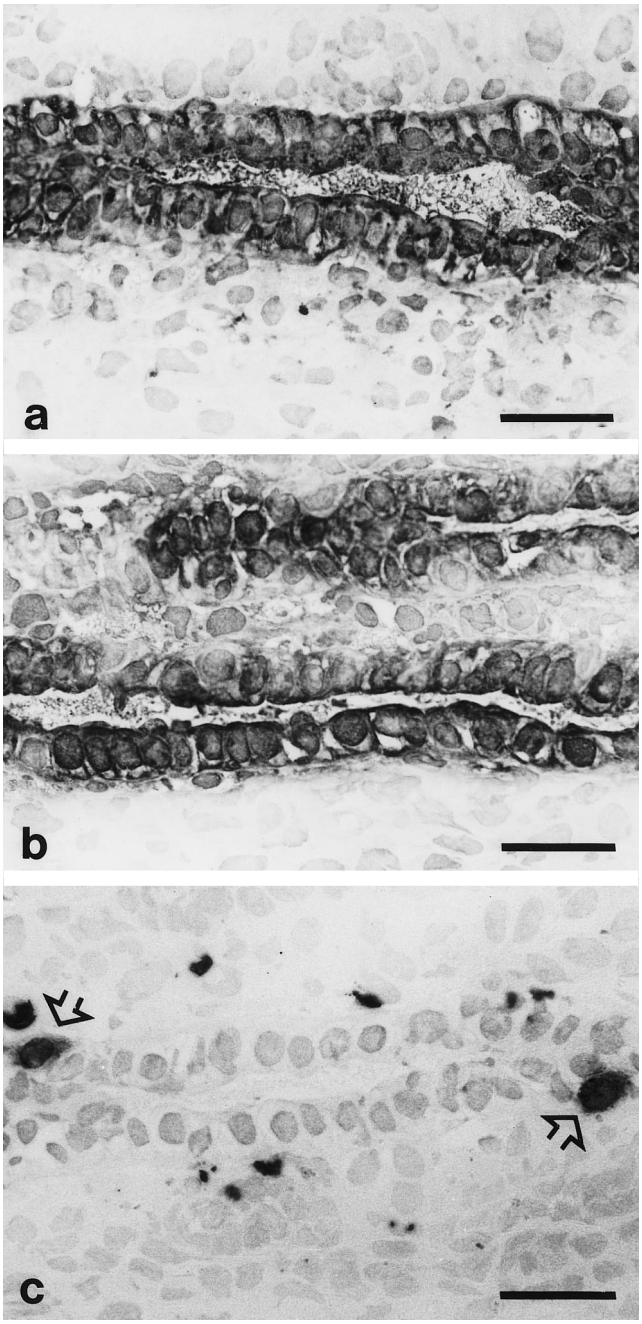

Fig. 4a–c Immunohistochemical characteristics of the CD epithlium of the neonatal rabbit kidney. All cells of the neonatal CD located beyond the transition zone were labelled by the monoclonal antibodies $P_{CD}6$, $P_{CD}8$, and $P_{CD}9$. All cells displayed homogeneous labelling. No restriction to the apical or basolateral membranes was observed. **a** $P_{CD}6$ bound to all the cells of the neonatal CD. **b** All the cells of the neonatal CD were labelled by $P_{CD}9$. **c** Within the midcortical region of the neonatal kidney and at the border between cortex and medulla very few cells (*open arrow*) were detected which expressed the band 3 protein. The antibody labelling showed a diffuse distribution. *Scale bar*, 25 µm

Antigen distribution of the neonatal CD beyond the ampullary region

The collecting tubule beyond the transition zone showed homogeneous labelling with the P_{CD} antibodies (Fig. 4). All of the cells of the midcortical and medullary CD were positive after incubation with these antibodies. $P_{CD}9$ antigen was continuously expressed by embyonic and more highly developed CD cells (Fig. 4b), while $P_{CD}6$ (Fig. 4a) and $P_{CD}8$ antigens were upregulated during the maturation of the epithelium. The antibodies $P_{CD}6$ and 8 are suitable for distinguishing between embryonic and maturing cells. These antigens were not expressed in the region of the embryonic ampullary tip, but were detectable in high concentrations below the ampullary neck (Fig. 3b).

Another example of a gradual increase in the expression of a protein during development can be demonstrated using the antibody IVF12. While none of the ampullary cells showed a positive reaction with the anti-Cl/HCO_3 exchanger antibody, up to 10% of epithelial cells from the midcortical to the medullary part were diffusely labelled by IVF12 (Fig. 4c).

Protein expression pattern of the adult CD epithelium

The development of the rabbit kidney is complete within 3–5 weeks after birth [35, 44]. Therefore, kidneys from animals older than 6 months were used for our investigations on antigen expression of the mature CD. Immunolabelling of the adult kidney revealed unexpected results (Figs. 5–7).

The $P_{CD}9$ antigen expressed by all epithelial cells of the embryonic and neonatal CD was downregulated by distinct cells of the mature CD (Fig. 5b). Regional differences in $P_{CD}9$ expression were monitored (Fig. 8). The CD of the inner medulla almost continuously expressed the $P_{CD}9$ antigen. $P_{CD}9$-negative cells were seldom found. Approximately 30% $P_{CD}9$-negative cells were counted within the outer medulla. Completely labelled segments were not found in this region. In contrast, the CD epithelium of the outer and inner cortex showed a considerable heterogeneity with respect to $P_{CD}9$ expression. The number of $P_{CD}9$ unlabelled cells in the outer and inner cortex varied over a wide range between 4% and 33%. In the outer cortex, epithelial segments were found where $P_{CD}9$-negative cells were nearly absent. In summary, $P_{CD}9$ expression was highly variable in the cortex region while the medullary parts of the CD were characterized by a constant expression pattern. Inner and outer medulla differed considerably with respect to the number of $P_{CD}9$-negative cells. The CD epithelium of the inner medulla showed nearly 100% $P_{CD}9$ expression, while in the outer medulla a relatively constant number of $P_{CD}9$-negative cells were detected.

A different expression pattern was observed for the $P_{CD}6$ antigen. First $P_{CD}6$ expression was upregulated in the neonatal CD. During final CD maturation, $P_{CD}6$ ex-

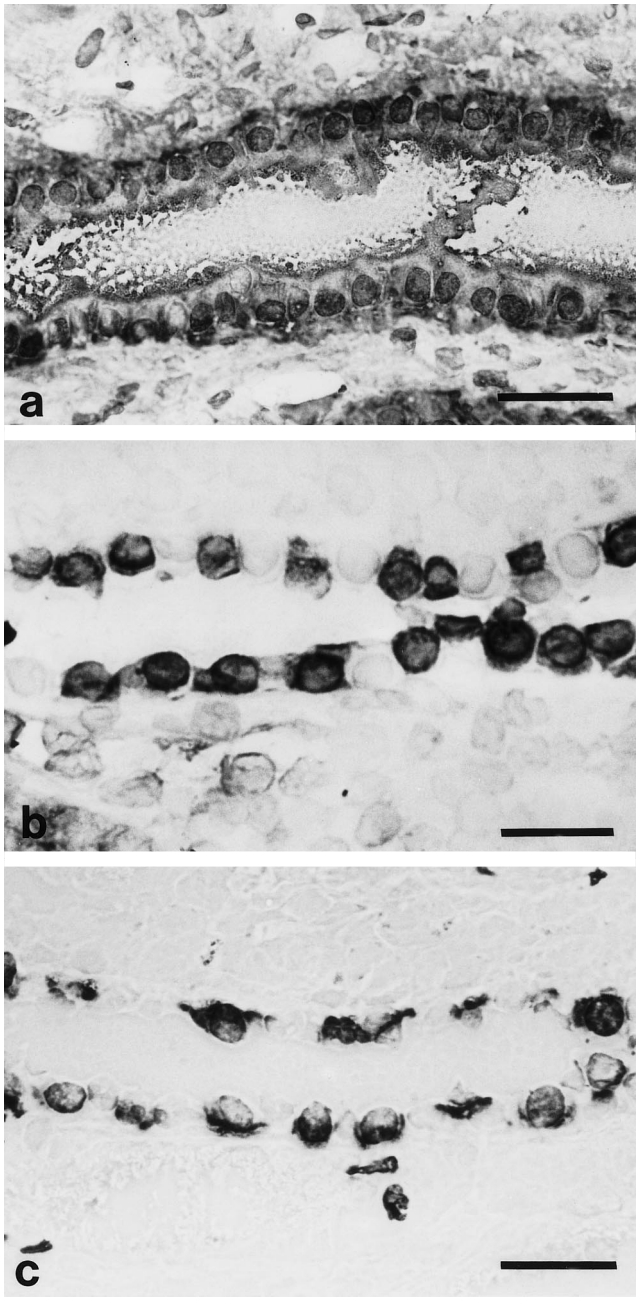

Fig. 5a–c Antigen expression pattern of the adult CD epithelium. For immune incubation, kidney sections from animals older than 6 months were used. **a** All cells of the mature CD were positive for $P_{CD}8$. A section through the medullar zone is shown. **b** The $P_{CD}9$ antigen was downregulated during maturation of the epithelium. Approximately 30% negative cells were counted along the CD of the outer medulla. **c** At the border between cortex and medulla 50% of the CD cells expressed the band 3 protein. These cells were characterized as α IC cells [51]. Labelling was restricted to the basolateral membranes of the differentiated cells. *Scale bar*, 25 μm

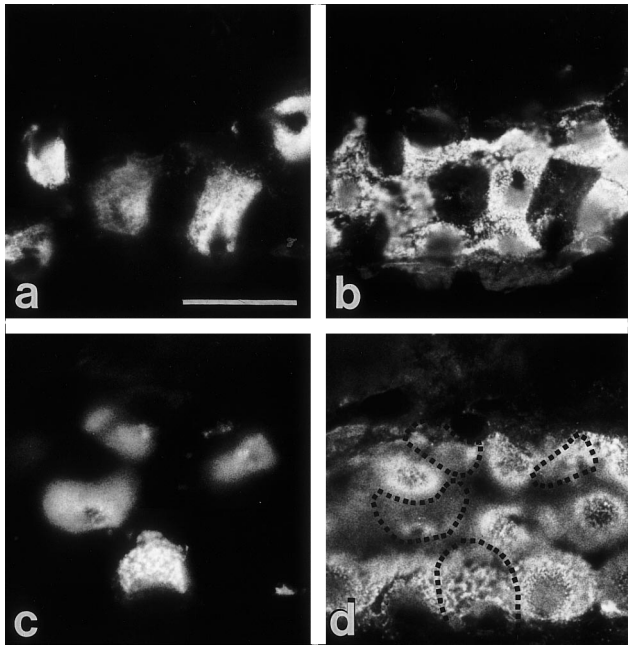

Fig. 6a–d CD cell subsets labelled by antibody $P_{CD}6$. Rhodamine-conjugated antibodies were utilized for the detection of $P_{CD}6$- labelled cells. Co-incubation experiments were carried out with fluorescein isothiocyanide (FITC)-coupled peanut agglutinin (PNA). The lectin PNA binds to β IC cells [33]. Different subsets of PNA-labelled cells were detected by co-incubation experiments. **a** CD segment of the midcortical region incubated with PNA. **b** Co-incubation of the same section with $P_{CD}6$ revealed that some of the PNA-labelled β IC cells did not express the $P_{CD}6$ antigen. **c** A section of the outer cortex region after PNA incubation. β IC cells were strongly labelled by PNA. **d** The section shown in **c** was co-incubated with $P_{CD}6$. This experiment revealed that a subset of β IC cells (*dotted lines*) expressed the $P_{CD}6$ antigen. *Scale bar*, 25 μm

pression was reduced. Approximately 10% of the mature cortical CD cells showed no immune reaction for this antigen (Table 2, Fig. 6b).

In contrast, two molecules were continuously upregulated during CD maturation. Both $P_{CD}8$ and the Cl/HCO_3 exchanger were not detectable in the embryonic ampulla, but all neonatal and adult CD cells expressed the $P_{CD}8$ antigen in large amounts (Fig. 5a). Thus, $P_{CD}8$ antibody is the first suitable marker for the differentiation of embryonic and differentiated CD cells.

The Cl/HCO_3 exchanger, a typical protein of α IC cells, also was upregulated during epithelial maturation. Compared with the neonatal CD, the number of Cl/HCO_3 exchanger-expressing α IC cells increased considerably: 11% positive cells were found in the cortical and 50% positive cells were seen in the medullary portion of the differentiated CD (Table 2, Fig. 5c) [51]. Antibody labelling was restricted to the basolateral membranes.

Characterization of $P_{CD}6$ and $P_{CD}9$ unlabelled cells

In order to investigate whether $P_{CD}6$- and $P_{CD}9$-negative cells might belong to the β-type IC cell population, co-incubation experiments were carried out using the lectin PNA as a label for β IC cells [33]. In the adult kidney, $P_{CD}6$-positive and $P_{CD}6$-negative cells were detected which reacted with PNA (Fig. 6). Not all of the PNA-

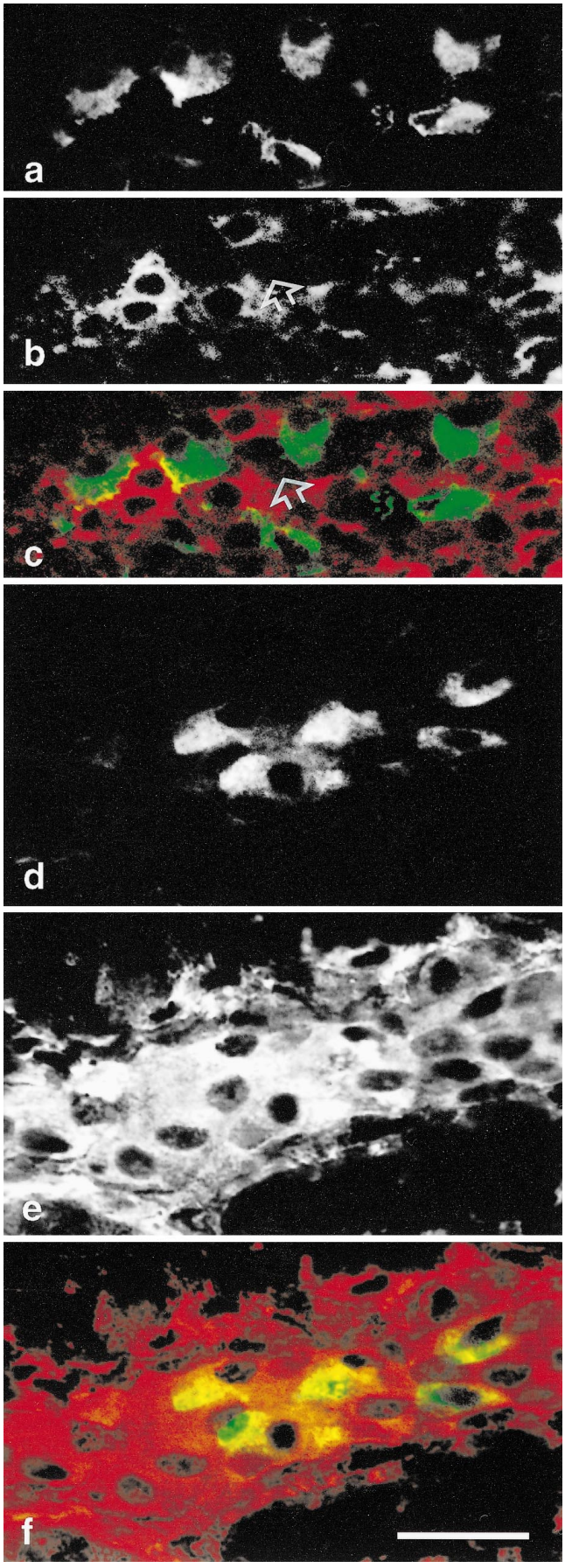

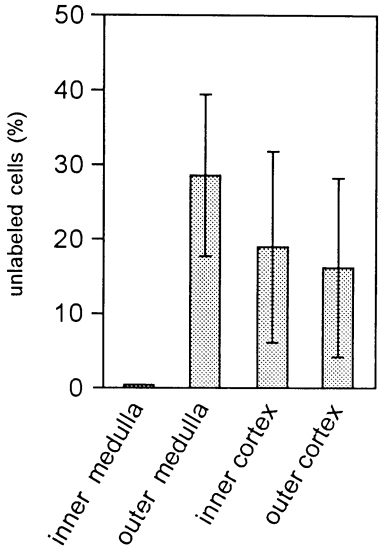

Fig. 8 Distribution of $P_{CD}9$-negative epithelial cells of the mature CD. Corticomedullary oriented sections of adult kidney were incubated with the antibody $P_{CD}9$. The number of $P_{CD}9$ unlabelled cells was counted in longitudinal sections of CD segments. Columns represent the percentage of unlabelled cells in the different zones of the CD (±SD)

binding β IC cells were labelled by $P_{CD}6$ (Fig. 6a, b). These results indicate a heterogeneous composition of the β IC cell subset.

The heterogeneity of the β IC cell population was confirmed after $P_{CD}9$ incubation. Again PNA labelling was detected on $P_{CD}9$-positive and on $P_{CD}9$-negative cells (Fig. 7). We conclude that this antigen was down-regulated by a proportion of the mature β IC cells. However, some of the $P_{CD}9$-negative cells proved also to be negative for PNA (Fig. 7a, c). The distribution of $P_{CD}9$-negative cells along the mature CD (Fig. 8) indicated that some of the P and α IC cells also reduced the expression of this antigen.

A characteristic distribution pattern of P and IC cells along the mature collecting tubule has been described [34, 44, 47]. The β IC cells, which can be distinguished by PNA binding from P and α IC cells, were most abun-

Fig. 7a–f Heterogeneity of the β IC cell population. Sections co-incubated with $P_{CD}9$ and PNA were analyzed by laser scan microscopy. β IC cells of the CD were detected by lectin labelling. The co-incubation experiments revealed that the β IC cell population is heterogeneous with respect to $P_{CD}9$ antigen expression. **a–c** Lectin-binding CD cells that did not express the $P_{CD}9$ antigens. **a** An optical section of the CD of the inner cortex is shown. Six cells were labelled by the FITC-coupled lectin. **b** Most cells of this CD section were labelled by the antibody $P_{CD}9$. Few were negative for $P_{CD}9$ (*arrow*). **c** The projection of **a** and **b** revealed that all PNA-binding cells (*green*) in this segment were not labelled by $P_{CD}9$ (*red*). Some $P_{CD}9$-negative cells were also negative for PNA (*arrows* in **a** and **b**). **d–f** CD cells are shown which were double-labelled by $P_{CD}9$ and PNA. **d** Five PNA-binding cells of the CD are shown. **e** All cells of this cortical CD segment were labelled by $P_{CD}9$. **f** The lectin-binding cells were also positive for $P_{CD}9$ labelling as indicated by the yellow color which resulted from the super imposing the *green* and *red* fluorescence. *Scale bar* 25 µm

dant in the outer cortex and the midcortical region [33, 44]. In contrast, α IC cells were the dominant cell type at the border between the cortex and the medulla [51]. A comparison of the reaction pattern of the new P_{CD} antibodies with the reported data on the typical distribution of P and IC cells showed only a poor correlation. None of the cloned antibodies was specific for one of the described cell types of the CD. $P_{CD}9$-negative cells were found along the CD from the outer medulla to the outer cortex. At the border between cortex and medulla, about 10% of the CD cells had downregulated the $P_{CD}6$ antigen. The cells which downregulated the P_{CD} antigens could not be associated exclusively with any of the described CD cell types.

Discussion

The heterogeneous composition of the mature CD epithelium was demonstrated by morphological [32, 51, 52] and physiological experiments [47] (Table 1). A model has been proposed explaining the different data with the existence of at least three distinct cell types. As mentioned by Schuster et al. [46], species differences have to be taken into account when applying this model of the CD system to different mammals.

In the rabbit kidney, α IC cells can be detected by the antibody IVF12, which binds to the Cl/HCO_3 exchanger, also known as band 3 protein [22]. The lectin PNA is frequently used as a marker for β IC cells of the rabbit [33]. Antibodies binding exclusively to P cells are not available for rabbit CD epithelium. To date no molecules have been found which are exclusively expressed by one of the CD cell types. Cross-reactions of CD-detecting antibodies with other cell types, such as those observed with some of our P_{CD} antibodies, are fairly common. Na/K-ATPase [41], carbonic anhydrase [13], and band 3 protein [22] are abundant in different cells and tissues. Their expression is not restricted to the cells of the CD epithelium.

The three cell types of the CD documented to date fulfill different functions, but they express a number of common proteins (Table 1). These results are confirmed by the binding pattern of some of the newly developed P_{CD} antibodies (Figs. 3–7). The $P_{CD}8$ antigen was detected on all maturing and differentiated cells of the CD epithelium. All the cells of the epithelium except those of the ampullary tip were labelled by $P_{CD}8$ this enables us for the first time to make a clear-cut distinction between the ampullary cells that are responsible for nephron induction and those parts of the CD that have already started to develop the features of the differentiated epithelium. It will be a helpful tool for cell culture experiments dealing with CD cells. The unique binding characteristics of $P_{CD}8$ allows for the discrimination between differentiation and dedifferentiation under culture conditions.

Another antigen co-expressed by the different cell types of the CD was detected by antibody $P_{CD}9$. The antibody $P_{CD}9$ labelled all of the ampullary and neonatal CD cells. Negative cells were only found in the adult kidney. $P_{CD}9$ unlabelled cells were detected along the CD from the outer medulla to the cortical region. Within the inner medulla, $P_{CD}9$-negative cells were extremely scarce. In contrast, in the outer medulla approximately 30% of the mature CD cells were negative for $P_{CD}9$. The cortical region was characterized by a more-variable expression of the $P_{CD}9$ antigen. Almost completely labelled duct segments were located beside segments with 30% unlabelled cells.

The distribution of $P_{CD}9$ unlabelled cells along the CD showed no correlation with the distribution of the different CD cell types. P cells are found along the whole CD [10, 54], while both types of IC cells are restricted to the outer medulla and the cortical region. The number of α IC cells is highest in the outer medulla (50% of the CD cells) [6, 51]. β IC cells prevail in the inner cortical zone (30% of the CD cells), while only 11% IC cells of the α-type are found here [6, 34, 51, 52].

We tried to further characterize the $P_{CD}9$-negative cell population. By PNA co-incubation experiments we demonstrated that a proportion of the $P_{CD}9$-negative cells belong to the β IC cell population. However, double-negative cells were also detected. At present we cannot specify whether these cells are of the P or the α IC cell type. For the β IC cell type, a heterogeneous expression was also detected for the $P_{CD}6$ antigen. Again $P_{CD}6$-positive as well as $P_{CD}6$-negative PNA-labelled cells were found. However, our results indicated that at least the β IC cell population is heterogeneously composed with respect to $P_{CD}6$ and $P_{CD}9$ antigen expression. These data can be interpreted in different ways.

It is conceivable that the $P_{CD}9$ antigen is important for the regulation of CD cells function. The two-dimensional electrophoretic separation of the $P_{CD}9$ antigen revealed a suspicious spot pattern of the 39-kDa variant (Fig. 2b), indicating a different post-translational modification of the protein. The molecular weight remained unaffected by this modification, while the isoelectric points varied in a range from 6.3 to 6.9. A comparable pattern is achieved by differential protein phosphorylation that is a common regulation mechanism for enzyme activity [49] or signal transducing receptors [24]. Due to its intriguing spot pattern in immunoblots and its distribution along the CD (Fig. 8), we speculate that $P_{CD}9$ might be involved in the regulation of specific cellular activities, as has recently been reported for several phosphatases during nephrogenesis [48]. $P_{CD}9$ might be a regulatory molecule expressed in all physiologically active CD cells. At present we have no further information about the post-translational modification of the $P_{CD}9$ antigen. Detailed analysis of the $P_{CD}9$ antigen is needed to further elucidate its function.

Another explanation for the outcome of our co-incubation experiments may be that more than three cell types establish the epithelium of the mature CD. It was proposed earlier by other authors [21, 14] that more than three different cell types are abundant in the CD. Recently a subpopulation of β IC cells was described [14].

These PNA-positive cells were named γ IC cells. According to immunohistological findings they express a Cl/HCO_3 exchanger molecule that differs from the band 3 protein [2]. The origin and function of this subpopulation of IC cells is unknown. In the past cells exhibiting a diffuse cytoplasmic distribution of the Cl/HCO_3 exchanger were thought to be transitional forms between α and β IC cells [16]. It was assumed that some of these cells may represent precursors responsible for the regeneration of the epithelium [9, 16]. Other authors have proposed that a functional plasticity of the CD may be achieved by converting the specific functions of the different cell types [5]. Our results gave further evidence for a hetergeneous composition of the β IC cell population. At present it is unknown whether this heterogeneity reflects a different state of cellular activity within this cell population or whether it is a further indication for an additional IC cell subset.

Morphological criteria indicate that the transition zone of the ampulla is mainly composed of mature CD cells [3, 4]. These results are in contradiction to the physiological data. The functional differentiation of the rabbit kidney takes place within 6 weeks after birth [25, 35, 43, 44]. The capability to concentrate the urine is not completely developed in newborn mammals [11]. Due to restricted HCO_3 secretion neonatal rabbits show a metabolic alkalosis [35].

It is well known that the CD's capability to reabsorb Na depends on postnatal maturation [20, 36, 50]. In neonatal kidney a high passive efflux of Na ions was measured which decreased gradually during the first 2 weeks of postnatal life [50]. Independently of the Na/K-ATPase expression found in all cells of the maturing CD [20], Na reabsorption tends to increase when tight junctions consisting of multiple strands have been formed. These reports are in close agreement with the results described in this paper. The functional maturation of the epithelium is reflected by distinct immunolabelling patterns. The CD epithelium of adult rabbits showed an antibody-binding pattern that can easily be distinguished from that of the neonatal as well as the ampullary duct (Figs. 3–5). Up- and downregulation of different proteins were detected during CD maturation. The expression of the $P_{CD}8$ antigen starts when the epithelial function converts from an embryonic inducer to the maturing CD. The first α IC cells are detected at the border between the cortex and the medulla of the neonatal kindey. Both immunolabelling and α IC cell numbers differ considerably from the situation found in the mature organ (Fig. 4) [25, 51]. While less than 10% of the cells in the neonate expressed the Cl/HCO_3 exchanger, 50% positive IC cells were detectable at the border between cortex and medulla in the differentiated CD. Immunolabelling was localized basolaterally in the adult, while the maturing cells were characterized by diffuse antibody binding.

While the maturation of α IC cells was characterized by enhanced expression of the Cl/HCO_3 exchanger, the differentiation of β IC cells was accompanied by a downregulation of protein expression. Both $P_{CD}9$ and $P_{CD}6$ antigen were expressed by all neonatal cells, even those labelled by PNA. In the adult kidney, co-localization of $P_{CD}9$ and PNA binding was restricted to a proportion of the β IC cells. The $P_{CD}9$ antigen was downregulated by a subset of the β IC cells. Furthermore, a proportion of β IC cells also had reduced $P_{CD}6$ expression. The diminished expression of an epithelial protein by IC cells has already been reported [20, 25]. In the prenatal kidney Na/K-ATPase is abundant in all cells of the CD, while it is downregulated postnatally in IC cells [41]. The downregulation of this protein is of functional significance, as has been described by Schuster et al. [46]. P cell function is correlated with the regulation of the Na/K balance, while IC cells are involved in the maintenance of the acid/base status of body fluids. However, we do not know whether the downregulation of $P_{CD}6$ and $P_{CD}9$ in a proportion of β IC cells is coupled with the functional maturation of these cells. Analyzing the distribution of $P_{CD}9$ unlabelled cells, it became obvious that P and α IC cells are also capable of downregulating this antigen. These results may be interpreted in terms of a functional plasticity of the CD epithelium [5]. The reduced expression of $P_{CD}9$ might be coupled to a distinct activation state of the mature CD cells. Further biochemical characterization of the $P_{CD}9$ antigen is under way in order to investigate the function of this molecule. The results presented herein reveal clear-cut morphological and immunohistological differences during CD maturation. The adult CD can be distinguished from the neonatal as well as from the ampullary duct epithelium. We conclude that the neonatal CD epithelium represents a transient differentiation stage.

Acknowledgements The skillful technical assistance of Mrs. Marion Kubitza and Mrs. Elfriede Eckert is gratefully acknowledged. We thank Mr. U. de Vries for his support in laser scan analysis. We are indebted to Dr. J. Monzer for the excellent graphic work. This investigation was supported by the Deutsche Forschungsgemeinschaft (Mi 331/4-1).

References

1. Adelsberg JS van, Edards JC, Herzlinger D, Cannon C, Rater M, Al-Awqati Q (1989) Isolation and culture of HCO_3-secreting intercalated cells. Am J Physiol 256:C1004–C1011
2. Adelsberg JS van, Edwards JC, al-Awqati Q (1993) The apical Cl/HCO_3 exchanger of beta intercalated cells. J Biol Chem 268:11283–11289
3. Aigner J, Kloth S, Kubitza M, Kashgarian M, Dermitzel R, Minuth WW (1994) Maturation of renal collecting duct cells in vivo and under per fusion culture. Epithelial Cell Biol 3:70–78
4. Aigner J, Kloth S, Jennings ML, Minuth WW (1995) Transitional differentiation patterns of principal and intercalated cells during renal collecting duct development. Epithelial Cell Biol 4:121–130
5. Al-Awqati Q (1996) Plasticity in epithelial polarity of renal intercalated cells: targeting of the H^+-ATPase and band 3. Am J Physiol 270:C1571–C1580
6. Alper SL, Natale J, Gluck S, Lodish HF, Brown D (1989) Subtypes of intercalated cells in rat kidney collecting duct defined by antibodies against erythroid band 3 renal vacuolar H+-ATPase. Proc Natl Acad Sci USA 86:5429–5433

7. Benos DJ, Saccomani G, Brenner BM, Sariban-Sohraby S (1986) Purification and characterization of the amiloride-sensitive sodium channel from A6 cultured cells and bovine renal papilla. Proc Natl Acad Sci USA 83:8525–8529
8. Breton S, Alper SL, Gluck SL, Sly WS, Barker JE, Brown D (1995) Depletion of intercalated cells from collecting ducts of carbonic anhydrase II-deficient (CAR2 null) mice. Am J Physiol 269:F761–F774
9. Brière N, Magny P (1993) Scanning electron microscopic observations of human fetal kidney maturing in vivo and in serum-free organ culture. Anat Rec 7:461–474
10. Brown D, Sorscher EJ, Ausiello DA, Benos DJ (1989) Immunocytochemical localization of Na channels in rat kidney medulla. Am J Physiol 256:F366–F369
11. Calgano PL, Rubin MI, Weintraub DH (1954) Studies on the renal concentrating and diluting mechanisms in the premature infant. J Clin Invest 33:91–96
12. Dorup J, Maunsbach AB (1982) The ultrastructural development of distal nephron segments in the human fetal kidney. Anat Embryol (Berl) 164:19–41
13. Edwards Y (1990) Structure and expression of mammalian carbonic anhydrases. Biochem Soc Trans 18:171–175
14. Emmons C, Kurtz I (1994) Functional characterization of three intercalated cell subtypes in the rabbit outer cortical collecting duct. J Clin Invest 93:417–423
15. Evan AP, Satlin LM, Gattone VH II, Connors B, Schwartz GJ (1991) Postnatal maturation of rabbit renal collecting duct. II. Morphological observations. Am J Physiol 261:F91–F107
16. Fejes-Tóth G, Náray-Fejes-Tóth A (1993) Differentiation of intercalated cells in culture. Pediatr Nephrol 7:780–784
17. Gandhi R, LeHir M, Kaissling B (1990) Immunolocalization of ecto-5′-nucleotidase in the kidney by a monoclonal antibody. Histochemistry 95:165–174
18. Gilbert P, Mundel P, Minuth WW (1990) Production of monoclonal antibodies against principal cells of the renal collecting duct by in vitro immunization with soluble antigens. J Histochem Cytochem 38:1919–1925
19. Herzlinger D (1994) Renal stem cells and the lineage of the nephron. Annu Rev Physiol 56:671–689
20. Holthöfer H (1987) Ontogeny of cell type-specific enzyme reactivities in kidney collecting ducts. Pediatr Res 22:504–508
21. Jamous M, Bidet M, Tauc M, Koechlin N, Gastineau M, Wanstok F, Poujeol P (1995) In young primary cultures of rabbit kidney cortical collecting ducts intercalated cells originate from principal or undifferentiated cells. Eur J Cell Biol 66:192–199
22. Jennings ML, Anderson MP, Monaghan R (1986) Monoclonal antibodies against human erythrocyte band 3 protein: localization of proteolytic cleavage sites and stilbene disulfonate-binding lysine residues. J Biol Chem 261:9002–9010
23. Jokelainen P (1963) An electron microscope study of the early development of the rat metanephric nephron. Acta Anat (Basel) [Suppl] 47:6–71
24. Karin M (1992) Signal transduction from cell surface to nucleus in development and disease. FASEB J 6:2581–2590
25. Kim J, Tisher CC, Madsen KM (1994) Differentiation of intercalated cells in developing rat kidney: an immunohistochemical study. Am J Physiol 266:F977–F990
26. Kloth S, Meyer D, Röckl W, Miettinen A, Aigner J, Schmidbauer A, Minuth WW (1992) Characterization of an endothelial protein in the developing rabbit kidney. Differentiation 52:79–88
27. Kloth S, Aigner J, Brandt E, Moll R, Minuth WW (1993) Histochemical markers reveal an unexpected heterogeneous composition of the renal embryonic collecing duct epithelium. Kidney Int 44:527–536
28. Koehler G, Milstein C (1975) Continuous cultures of fused cells secreting antibody of predefined specificity. Nature 256: 495–497
29. Koeppen BM (1987) Electrophysiological identification of principal and intercalated cells in the rabbit outer medullary collecting duct. Pflügers Arch 409:138–141
30. Kujat R, Rose C, Wrobel KH (1993) The innervation of the bovine ductus deferens: comparison of a modified acetylcholinesterase-reaction with immunoreactivities of cholintransferase and pan-neuronal markers. Histochemistry 99:231–239
31. Laemmli UK (1970) Cleavage of structural proteins during assembly of the head of bacteriophage T4. Nature 227:680–685
32. Le Furgey A, Tisher CC (1979) Morphology of rabbit collecting duct. Am J Anat 155:111–124
33. LeHir M, Kaissling B, Koeppen BM, Wade JB (1982) Binding of peanut lectin to specific epithelial cell types in the kidney. Am J Physiol 242:117–120
34. Madsen KM, Verlander JW, Linser PJ, Tisher CC (1989) Identification of intercalated cells in rabbit medullary collecting duct. Kidney Int 35:458–465
35. Mehrgut FM, Satlin LM, Schwartz GJ (1990) Maturation of HCO_3- transport in rabbit collecting duct. Am J Physiol 259:F801–F808
36. Minuth WW, Gross P, Gilbert P, Kashgarian M (1987) Expression of the α-subunit of Na/K-ATPase in renal collecting duct epithelial during development. Kidney Int 31:1104–1112
37. Minuth WW, Gilbert P, Rudolph U, Spielman WS (1989) Successive histochemical differentiation steps during postnatal development of the collecting duct in rabbit kidney. Histochemistry 93:19–25
38. Moll R, Hage C, Thoenes W (1991) Expression of intermediate filament proteins in fetal and adult human kidney: modulation of intermediate filament patterns during development and in damaged tissue. Lab Invest 65:74–86
39. Neiss WF (1982) Morphogenesis and histogenesis of the connecting tubule in the rat kidney. Anat Embryol (Berl) 165:81–95
40. O'Farrell P (1975) High resolution two-dimensional electrophoresis of proteins. J Biol Chem 250:4007–4021
41. Ridderstrale Y, Kashgarian M, Koeppen B, Giebisch G, Stetson D, Ardito T, Stanton B (1988) Morphological heterogeneity of the rabbit collecting duct. Kidney Int 34:655–670
42. Sariola H, Sainio K (1997) The tip-top branching ureter. Curr Opin Cell Biol 9:877–884
43. Satlin LM (1994) Postnatal maturation of potassium transport in rabbit cortical collecting duct. Am J Physiol 266:F57–F65
44. Satlin LM, Matsumoto T, Schwartz GJ (1992) Postnatal maturation of rabbit renal collecting duct. III. Peanut lectin binding intercalated cells. Am J Physiol 262:F199–F208
45. Saxén L (1987) Organogenesis of the kidney. In: Barlow PW, Green PB, Wylie CC (eds) Developmental and cell biology series, vol. 19. Cambridge University Press, Cambridge
46. Schuster VL (1993) Function and regulation of collecting duct intercalated cells. Annu Rev Physiol 55:267–288
47. Schuster VL, Bonsib SM, Jennings ML (1986) Two types of collecting duct mitochondria rich (intercalated) cells: lectin and band 3 cytochemistry. Am J Physiol 251:C347–C355
48. Svennilson J, Durbeej M, Celsi G, Laestadius A, Cruz e Silva EF da, Ekblom P, Aperia A (1995) Evidence for a role of protein phosphatase 1 and 2A during early nephrogenesis. Kidney Int 48:103–110
49. Taylor SS, Knighton DR, Zheng J, Ten-Eyck LF, Sowadski JM (1992) Structural framework for the protein kinase family. Annu Rev Cell Biol 8:429–462
50. Vehaskari VM (1994) Ontogeny of cortical collecting duct sodium transport. Am J Physiol 267:F49–F54
51. Verlander JW, Madsen KM, Low PS, Allen DP, Tisher CC (1988) Immunocytochemical localisation of band 3 protein in the rat collecting duct. Am J Physiol 255:F115–F125
52. Verlander JW, Madsen KM, Stone DK, Tisher CC (1994) Ultrastructural localization of H^+-ATPase in rabbit cortical collecting duct. J Am Soc Nephrol 4:1546–1557
53. Weiner ID, Hamm L (1990) Regulation of intracellular pH in the rabbit cortical collecting tubule. J Clin Invest 85:274–281
54. Yasui M, Marples D, Belusa R, Eklof AC, Celsi G, Nielsen S, Aperia A (1996) Development of urinary concentration capacity: role of aquaporin-2. Am J Physiol 271:F461–F468